

# Two-Photon Calcium Imaging Reveals an Odor-Evoked Map of Activity in the Fly Brain

Jing W. Wang,<sup>1</sup> Allan M. Wong,<sup>1</sup> Jorge Flores,<sup>1</sup> Leslie B. Vosshall,<sup>2</sup> and Richard Axel<sup>1,\*</sup>

<sup>1</sup>Department of Biochemistry and Molecular Biophysics

Howard Hughes Medical Institute  
College of Physicians and Surgeons  
Columbia University  
701 West 168th Street  
New York, New York 10032

<sup>2</sup>Laboratory of Neurogenetics and Behavior  
The Rockefeller University  
New York, New York 10021

## Summary

An understanding of the logic of odor perception requires a functional analysis of odor-evoked patterns of activity in neural assemblies in the brain. We have developed a sensitive imaging system in the *Drosophila* brain that couples two-photon microscopy with the specific expression of the calcium-sensitive fluorescent protein, G-CaMP. At natural odor concentration, each odor elicits a distinct and sparse spatial pattern of activity in the antennal lobe that is conserved in different flies. Patterns of glomerular activity are similar upon imaging of sensory and projection neurons, suggesting the faithful transmission of sensory input to higher brain centers. Finally, we demonstrate that the response pattern of a given glomerulus is a function of the specificity of a single odorant receptor. The development of this imaging system affords an opportunity to monitor activity in defined neurons throughout the fly brain with high sensitivity and excellent spatial resolution.

## Introduction

For most animals, smell is the central sensory modality affording the organism the ability to detect food, predators, and mates. *Drosophila* provides an attractive system to understand the logic of olfactory perception because flies exhibit complex behaviors controlled by an olfactory system that is anatomically and genetically simpler than that of vertebrates. Genetic analysis of olfaction in *Drosophila* may therefore provide a facile system to understand the mechanistic link between behavior and the perception of odors.

Olfactory perception requires the recognition of a diverse repertoire of odorous molecules in the periphery and more central neural mechanisms that allow the discrimination of odors and appropriate behavioral responses. The recognition of odors in *Drosophila* is accomplished by sensory hairs distributed over the surface of the third antennal segment and the maxillary palp. Olfactory neurons within sensory hairs send projections to one of 43 glomeruli within the antennal lobe of

the brain (Stocker, 1994; Laissue et al., 1999). Individual sensory neurons are likely to express only one of about 80 odorant receptor genes (Clyne et al., 1999; Vosshall et al., 1999; Gao and Chess, 1999; Vosshall et al., 2000; Scott et al., 2001; Dunipace et al., 2001) and 80% of the neurons also express a common receptor gene, *Or83b* (Vosshall et al., 2000). Neurons expressing the same receptors project with precision to one or rarely two spatially invariant glomeruli within the antennal lobe (Gao et al., 2000; Vosshall et al., 2000; Scott et al., 2001).

The anatomic organization in *Drosophila* is remarkably similar to that of the olfactory system of mammals (Mombaerts, 1999; Vosshall, 2000), suggesting the mechanism of odor discrimination has been shared, despite the five hundred million years of evolution separating insects from mammals. The convergence of like axons into discrete glomerular structures provides a map of receptor activation in the first relay station for olfactory information in the brain. An odorant could interact with multiple receptors resulting in the activation of a topographically invariant combination of glomeruli. The quality of an odorant may therefore be reflected by defined spatial patterns of activity, first in the antennal lobe or olfactory bulb, and ultimately in higher olfactory centers in the brain.

How does the anatomic map translate into a functional map? Previous imaging studies in large insects and vertebrates demonstrate that different odors elicit defined spatial patterns of glomerular activation, revealing a functional representation of an anatomic map (Kauer et al., 1987; Friedrich and Korsching, 1997; Joerges et al., 1997; Galizia et al., 1999; Malnic et al., 1999; Rubin and Katz, 1999; Uchida et al., 2000; Wachowiak and Cohen, 2001; Meister and Bonhoeffer, 2001; Belluscio et al., 2002; Spors and Grinvald, 2002). In *Drosophila*, however, the topographic map is largely based upon anatomic studies that identify highly stereotyped patterns of connectivity from the antenna to the protocerebrum (Gao et al., 2000; Vosshall et al., 2000; Scott et al., 2001; Marin et al., 2002; Wong et al., 2002). We have employed a calcium-sensitive fluorescent protein (Miyawaki et al., 1997; Nakai et al., 2001) in concert with two-photon microscopy (Denk et al., 1990) to determine the relationship of the anatomic and the functional map in the antennal lobe of the fruit fly. We have expressed G-CaMP (Nakai et al., 2001) in primary olfactory sensory neurons and projection neurons (PNs). The ability to express G-CaMP in genetically defined populations of neurons allows us to determine with certainty the locus of neural activity. Odor-evoked changes in fluorescent intensity within the antennal lobe are monitored by a laser scanning two-photon microscope. Two-photon imaging causes less phototoxicity and permits deeper tissue penetration than other fluorescent microscopy techniques, providing high spatial and temporal resolution imaging of calcium influx in neurons (Yuste and Denk, 1995; Svoboda et al., 1997; Helmchen et al., 1999; Wang et al., 2000; Delaney et al., 2001; Wang et al., 2001).

We have developed an isolated *Drosophila* brain preparation that is amenable to two-photon imaging and is

\*Correspondence: ra27@columbia.edu

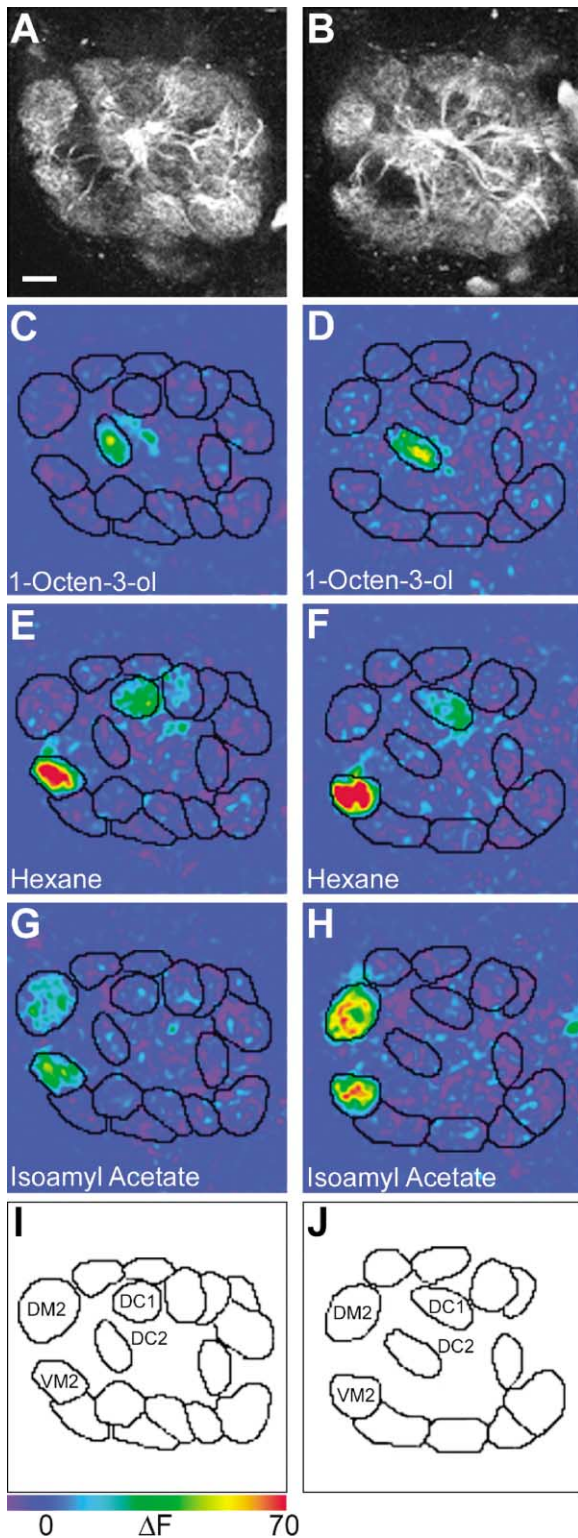


**Figure 1. The Pattern of Glomerular Activation in Response to the Same Odor Is Conserved among Different Organisms**

Preparations from two different flies bearing the *GH146-Gal4* and *UAS-GCaMP* transgenes were exposed to 1-octen-3-ol, hexane, and isoamyl acetate at 8% saturated vapor concentration (SV). The fluorescent intensity was monitored with a laser scanning two-photon microscope. The glomerular responses of two different specimens at similar optical planes are shown.

responsive to odor stimulation for up to five hours. In animals expressing G-CaMP in neurons of the olfactory system, the application of odors results in large increases in fluorescent intensity that permits imaging with a sensitivity and resolution not previously possible. These imaging experiments demonstrate that different odors activate different combinations of glomeruli and these spatial patterns of activity are conserved in different flies. At concentrations of odors reflective of the fly's native environment, the map is sparse with glomeruli narrowly tuned to a small number of molecular structures. Similar functional maps are obtained from images of either sensory axons or projection neuron dendrites. Misexpression of a specific odorant receptor demonstrates that the responsiveness of individual glomeruli is a consequence of the odorant sensitivity of the individual receptors. More generally, these imaging studies provide an experimental system to monitor activity in defined neurons throughout the fly brain with high sensitivity and fine spatial resolution.

## Results

### A Functional Map of Odor Activation in the Antennal Lobe

We have developed a preparation that permits the detection of odor-evoked changes in fluorescent intensity in the *Drosophila* antennal lobe by two-photon microscopy. The sensitivity of this imaging approach was initially examined by expressing G-CaMP (Nakai et al., 2001) in olfactory projection neurons. G-CaMP consists of a circularly permuted EGFP flanked on one side by the M13 fragment of myosin light chain kinase and on the other by the calcium binding site of calmodulin. In the presence of calcium, calmodulin interacts with the M13 fragment eliciting a conformational change in EGFP resulting in elevations in fluorescent intensity that reflect changes in the intracellular calcium concentration, a presumed mirror of electrical activity.

Two hundred projection neurons surround the antennal lobe (Stocker et al., 1990). The dendrites of most PNs innervate a single glomerulus, whereas the axons project to the calyx of the mushroom body and the protocerebrum (Stocker et al., 1990; Jefferis et al., 2001; Marin et al., 2002; Wong et al., 2002). An enhancer trap line, *GH146-Gal4*, has been characterized that drives the expression of *Gal4* in approximately 90 of the 200 PNs (Stocker et al., 1997; Jefferis et al., 2001). This subset of PNs innervates 34 of the 43 antennal lobe glomeruli (Laiusue et al., 1999). Flies that contain the *GH146-*

(A and B) Prestimulation images show glomerular structure. Scale bar = 10  $\mu$ m.

(C–H) The glomerular response to the three different odors in two different flies (C, E, and G versus D, F, and H). For each odor, 100 frames of images (128  $\times$  128 pixels for 96  $\times$  96  $\mu$ m field of view) were collected at a rate of 4 fps. Odorants were delivered for 2 s at the beginning of the tenth frame and  $\Delta$ F images were obtained by subtracting the averaged prestimulation image from each frame. The average of three frames surrounding the peak  $\Delta$ F response is shown for each odor.

(I and J) Specific glomeruli were identified anatomically using the previously established antennal lobe map (Laiusue et al., 1999).

*Gal4* and *UAS-GCaMP* transgenes express G-CaMP in the cell bodies, axons, and dendrites of the projection neurons allowing us to visualize individual glomeruli (Figures 1A and 1B).

Odor-evoked changes in the antennal lobe of these flies were detected in a preparation that maintains the integrity of the olfactory system and is amenable to analysis in the two-photon microscope. Briefly, the fly was decapitated, and the cuticle and connective tissue were removed from the head by microdissection to reveal the brain and attached antennae. The specimen was embedded in agarose gel, and the antennae were exposed to allow the quantitative delivery of odors via an olfactometer. This agarose-embedded preparation provided robust odor responses for up to five hours permitting multiple samplings of odor responsivity in the same preparation.

We have analyzed the response of 23 different glomeruli to 16 pure odorants at multiple concentrations. Two-photon imaging through 5 optical planes permits sampling of the entire antennal lobe and reveals that each odorant elicits a different pattern of glomerular activity that provides a unique representation of an odor. The signal-to-noise ratio is high with  $\Delta F/F$  reaching up to 120% in response to odors over a base line noise level of less than 4%. The spatial resolution ( $0.5 \times 0.5 \times 2 \mu\text{m}$ ) allows discrimination among neighboring glomeruli with confidence.

At low odor concentrations, the glomerular response is sparse. Exposure to three different odors, 1-octen-3-ol, hexane, and isoamyl acetate at 8% saturated vapor concentration (SV), reveals that each odor elicits a different pattern of glomerular activity and these patterns are conserved among different animals (Figure 1). At 2% SV, many odors fail to elicit a significant response and those that do activate a small number of glomeruli (Figures 1 and 3). At higher odor concentrations, the number of glomeruli activated by a given odor increases to reveal a dense map with individual odors activating from two to as many as 15 of the 23 glomeruli analyzed (Figures 2 and 3). The response to six odors at 33% SV results in a denser map with greater overlap. The VM2 and DM2 glomeruli for example respond to four or five of the six odors tested (Figure 2; also see movies of glomerular response in Supplemental Data available at <http://www.cell.com/cgi/content/full/112/2/271/DC1>).

We have analyzed the odor-evoked changes in fluorescent intensity as a function of increasing concentrations of isoamyl acetate (Figure 4). We constructed an olfactometer in which a separate airstream dilutes saturated vapor concentrations for a given odorant, allowing us to deliver accurate dilutions of odor at the antennae. Isoamyl acetate activates four glomeruli (DM2, VM3, DM3, and DL1) in one optical plane (Figure 4A). The response to increasing concentrations of isoamyl acetate was independently measured for each of these glomeruli. For each glomerulus  $\Delta F/F$  increases with odor concentration, but the four glomeruli exhibit different sensitivities to isoamyl acetate. Since the threshold response differs for each of the glomeruli, the number of activated glomeruli increases with odor concentration. Isoamyl acetate activates only 3 glomeruli at 2% SV and 15 glomeruli at 40% SV (Figure 3). Although the behavioral threshold for this odor has not been studied

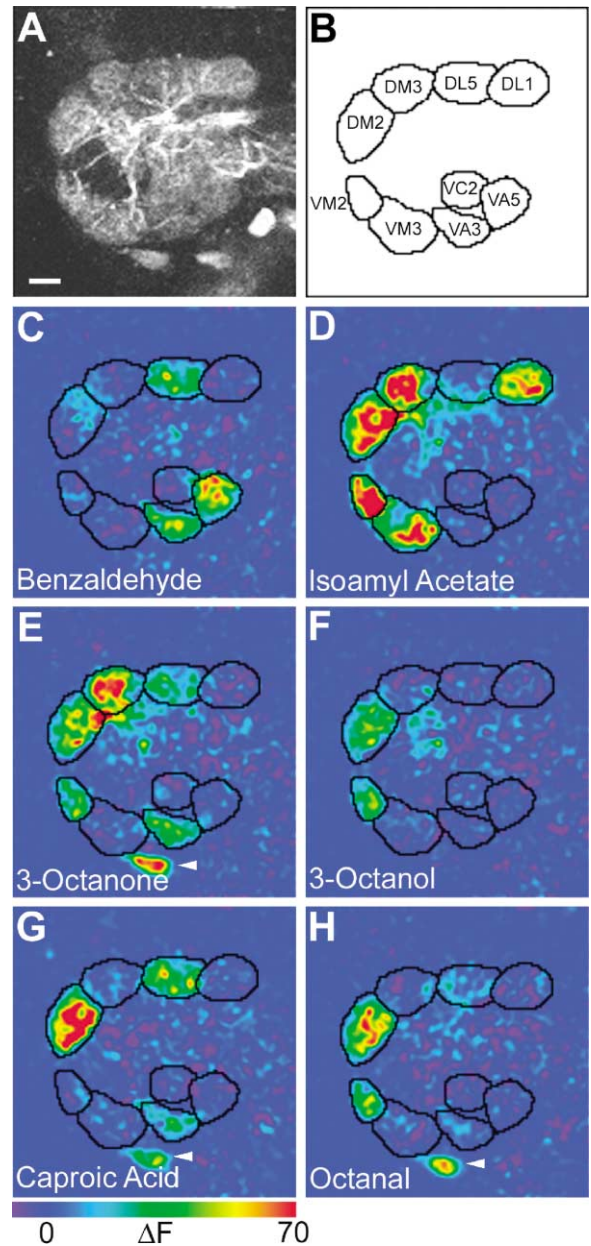


Figure 2. Different Odors Elicit Different Patterns of Glomerular Activation in the Antennal Lobe

A brain preparation from flies expressing G-CaMP in projection neurons was analyzed by two-photon imaging of the antennal lobe.

(A) A single optical plane through the antennal lobe reveals the glomerular structure. Scale bar = 10  $\mu\text{m}$ .

(B) Glomeruli in this optical plane were identified.

(C-H) Six different odorants were delivered to the antennae at 33% SV. The average of three frames surrounding the peak  $\Delta F$  response is shown for each odor. Caproic acid, 3-octanone, and octanal also activated the same PN cell body visible on this optical plane (arrowhead).

in the fruit fly, it is likely that these high odor concentrations are never experienced in the native environment. Thus, the sparse patterns observed are likely to more accurately reflect salient odor-evoked patterns in the fly antennal lobe.

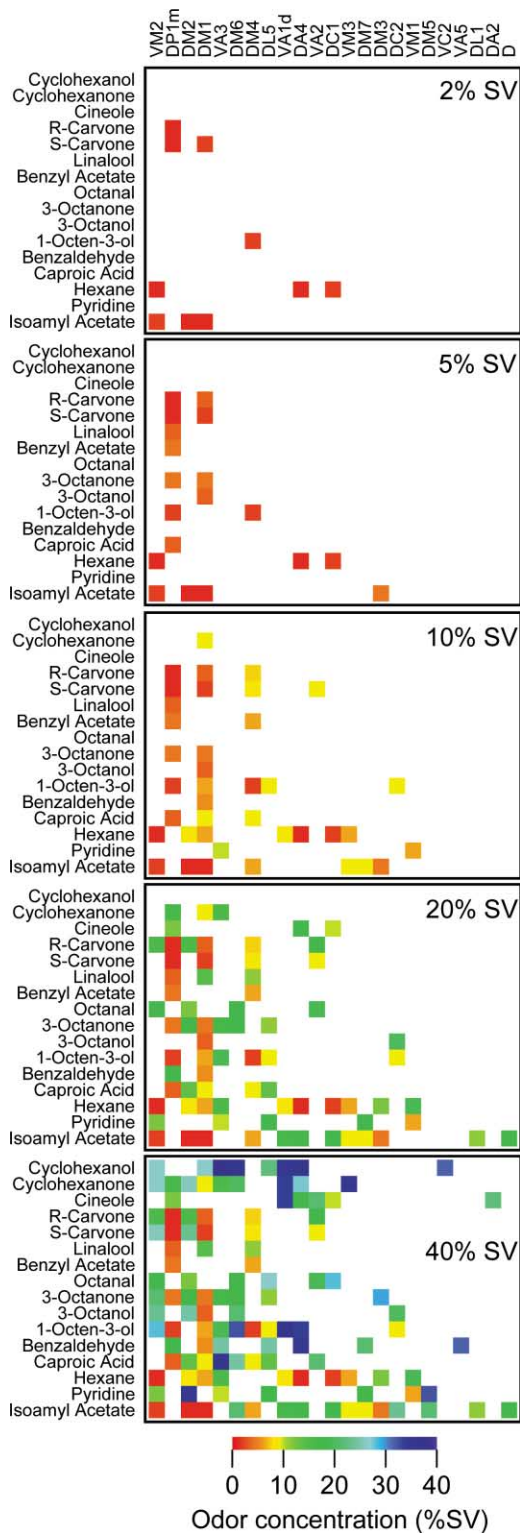


Figure 3. A Functional Map of Glomerular Activation in the Antennal Lobe

The responsivity of 23 glomeruli labeled by *GH146-Gal4* to 16 pure odorants was determined. Calcium influx was monitored in PN dendrites with G-CaMP. Multiple dilutions of the saturated vapor concentration for each odor were delivered to the antennae to determine the minimum concentration required to elicit a 20% change in  $\Delta F/F$  for a given glomerulus. At 2% SV, many odors tested failed to elicit

A number of interesting features of the glomerular response to odors are revealed by these initial experiments. Different odors elicit different patterns of glomerular activation and these patterns are conserved among different animals. At odor concentrations likely to be encountered in nature, the map is sparse and glomeruli are narrowly tuned. The map becomes denser at higher concentrations and glomeruli respond to multiple odors of widely different structures. The threshold of activation differs for different glomeruli so that the number of activated glomeruli increases with odor concentration. The patterns of activity are insular such that neighboring glomeruli do not necessarily respond together to a given odor. Each glomerulus visualized anatomically appears to be a functional unit. No partial activity is observed in subcompartments of the glomerular structure. Thus, these imaging results demonstrate that each odorant activates a sparse, conserved set of glomeruli that confers a signature for each odor in the brain.

### Quantitating the Glomerular Response

These imaging experiments rely on changes in fluorescent intensity as an indicator of odor-evoked responses. It is therefore important to determine the sensitivity of the changes in fluorescent intensity and to demonstrate that the odor-evoked responses are dependent upon odor concentration. We therefore attempted to correlate the sensitivity of  $Ca^{2+}$  imaging with spike frequency. A specimen was obtained from flies bearing *GH146-Gal4* and *UAS-GCaMP* transgenes, and the antennae were removed to allow electrical stimulation of the antennal nerve, rather than odor stimulation of the antennae. A brief stimulation of 1 ms duration was applied to the antennal nerve. Since single unit recording of sensory neurons in the fly reveals a monotonic response to odors (de Bruyne et al., 2001), it is likely that these short electrical pulses will generate only a single action potential in each axon. We monitored the change in fluorescent intensity ( $\Delta F/F$ ) after this stimulation paradigm for two glomeruli, DM2 and DL1, and observed a 10% increase in fluorescent intensity (at 2 mM extracellular  $Ca^{2+}$ ) when only a single stimulus was delivered to each sensory axon. Increasing the number of stimuli increases  $\Delta F/F$  with a maximum change in fluorescent intensity of 50% under these conditions (Figure 5D). Since an average glomerulus receives input from about 20 sensory axons, this imaging configuration potentially allows us to detect as few as 20 spikes arriving at a glomerulus simultaneously.

The observed responses result from changes in  $Ca^{2+}$  since no change in fluorescent intensity is recorded in the absence of extracellular  $Ca^{2+}$  (data not shown). Moreover, a 2-fold increase in extracellular  $Ca^{2+}$  results in close to an 8-fold increase in  $\Delta F/F$  (Figure 5D). A plot

a significant response and those that do activate a small number of glomeruli. At higher odor concentrations, the number of glomeruli activated by a given odor increased to reveal a dense map with individual odors activating from two for benzyl acetate to as many as 15 for isoamyl acetate. Each data point is the average odor concentration from 3–7 different samples. A total of 120 preparations were examined.

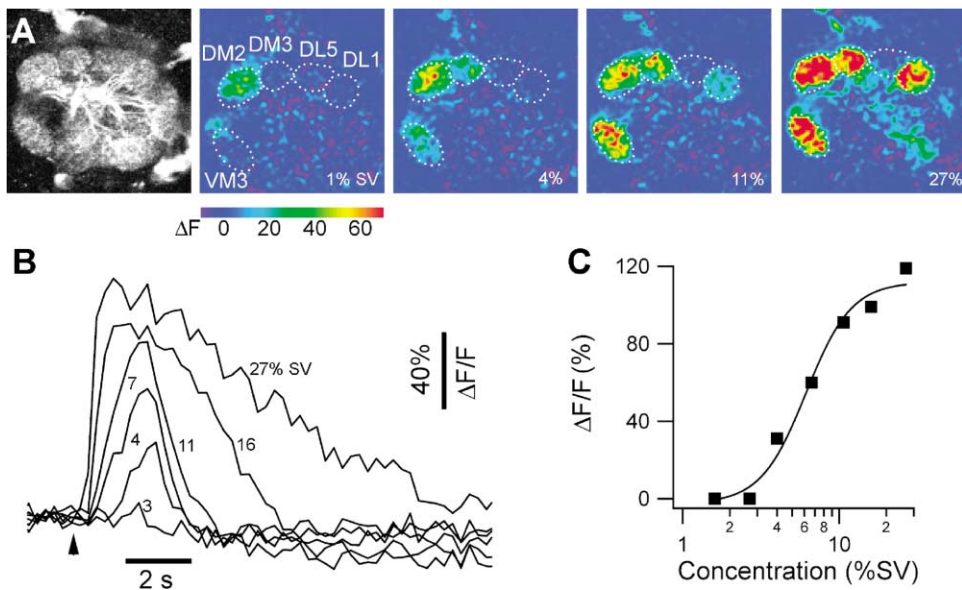


Figure 4. Concentration Dependence of the Glomerular Response to Isoamyl Acetate

(A) The average of prestimulation images is shown in grayscale to reveal the glomerular structure on one optical plane (left image). Peak responses to increasing concentrations of odor (left to right, 1%, 4%, 11%, and 27% SV) are shown in false-color scale. Each image is the average of three frames surrounding the peak  $\Delta F$  response.

(B) Time course of fluorescent change ( $\Delta F/F$ ) for the VM3 glomerulus at different odor concentrations. Increasing odor concentrations enhanced the change of fluorescent intensity and prolonged the time duration of the response. The decay time constants of  $\Delta F/F$  traces are 0.3, 0.4, 0.5, 1.1, 3.7, and 7.7 s for concentrations of isoamyl acetate at 3%, 4%, 7%, 11%, 16%, and 27% SV, respectively.

(C) The peak  $\Delta F/F$  of the VM3 glomerulus is plotted against odor concentration. Data from (B) were fitted by the Hill equation with a coefficient of 3.

of  $\Delta F/F$  as a function of the number of stimuli reveals a Hill coefficient of 3, a value similar to that observed when  $\Delta F/F$  is plotted against calcium concentration (Nakai et al., 2001), suggesting that post synaptic calcium influx in PN dendrites is linearly related to the number of stimuli.

#### Imaging Odor-Evoked Activation of Sensory Neurons

The imaging data presented above reflect odor-evoked activity within the dendrites of projection neurons. Activity within projection neurons in a given glomerulus could result from the firing of presynaptic sensory axons that directly synapse on PNs within a given glomerulus or from indirect inputs from recurrent connections or local interneurons. We have therefore performed imaging experiments that record odor-evoked changes in fluorescent intensity in presynaptic sensory termini to ask whether there is a correspondence between the activity patterns of input sensory neurons and output projection neurons. Imaging was performed on preparations in which G-CaMP is expressed in primary olfactory neurons rather than projection neurons. One member of the odorant receptor gene family, *Or83b*, is unique among the odorant receptor genes because it is expressed in 80% of the sensory neurons (Vosshall et al., 2000). Flies bearing the *Or83b-Gal4* transgene along with *UAS-GCaMP*, reveal expression of G-CaMP in most of the GH146-positive glomeruli (data not shown). These flies were then exposed to nine of the 16 odors used in previous experiments, and the spatial patterns of activity in sensory termini within the glomeruli were determined by two-photon imaging.

We have compared the patterns of glomeruli activated by caproic acid and isoamyl acetate in flies in which G-CaMP is expressed in either the sensory neurons or the projection neurons (Figure 6). The patterns of glomerular activity are qualitatively similar upon imaging either the sensory or projection neurons. However, the magnitude of odor-evoked increases in fluorescent intensity is often lower in the sensory versus projection neurons. This may reflect different levels of calcium elevation elicited in axons and dendrites or may simply result from technical differences in the levels of G-CaMP expression in the two different cell types.

We have performed a more extensive comparison of the responsivity of individual glomeruli to multiple different odors after imaging of sensory and projection neurons. Since the sensitivity of G-CaMP in sensory neurons is lower than in PNs, these studies were necessarily performed at higher odorant concentrations (36% SV). There is a striking concordance in their responses such that a given odor will activate the same glomeruli whether G-CaMP is expressed in sensory or projection neurons (Figure 6I). This concordance is apparent for nine odors activating 17 glomeruli suggesting that the activity we observe in PN directly reflects input from sensory fibers.

#### Imaging of the Projection Neuron Cell Bodies

We observe that the cell bodies of projection neurons expressing G-CaMP also show an increase in fluorescent intensity in response to odor stimulation. We selected two odorants, pyridine and hexane, that activate several glomeruli in the antennal lobe and examined the

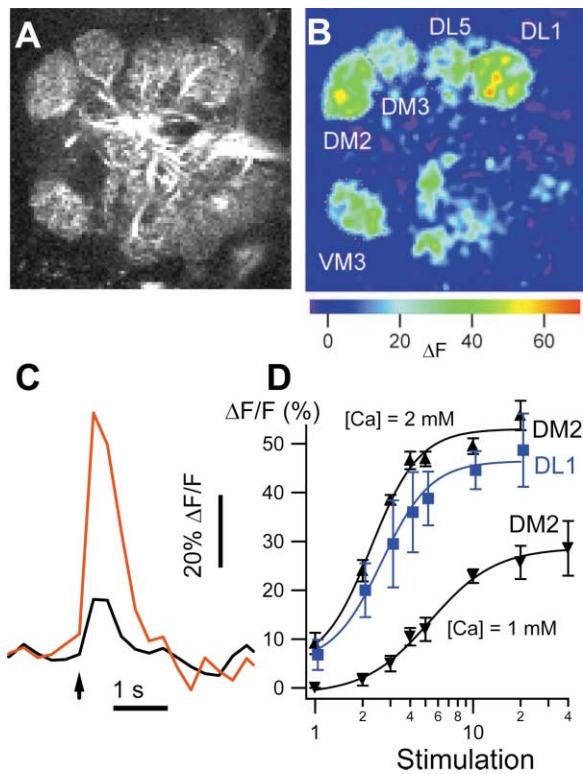


**Figure 5. The Change in Glomerular Fluorescent Intensity  $\Delta F/F$  Is Correlated with the Spike Frequency in the Antennal Nerve**

Antennae and cuticle were removed from a fly bearing the *GH146-Gal4* and *UAS-GCaMP* transgenes. The brain was immersed in saline and pinned down on a Sylgard plate. A suction electrode was used to stimulate the antennal nerve.

(A) The average of the prestimulation images reveals discrete and identifiable glomeruli.

(B) Five short electrical stimuli, 1 ms in duration and 10 V in amplitude, were delivered to the ipsilateral olfactory nerve at a frequency of 100 Hz.  $\Delta F$  image at the peak response is shown in false-color scale and reveals that the five identifiable glomeruli in this optical plane were responsive to electrical stimulation.

(C) Time course of change in fluorescent intensity ( $\Delta F/F$ ) in the DM2 glomerulus in response to 1 (black trace) and 5 (red trace) electrical stimuli. The arrow indicates the beginning of the electrical stimulation.

(D) Peak amplitude of  $\Delta F/F$  increases with the number of stimuli applied to the olfactory nerve. Averaged peak amplitude of  $\Delta F/F$  for the DM2 (black triangles) and DL1 (blue squares) glomeruli in response to different number of electrical stimuli. Each data point represents the average of  $\Delta F/F$  from 3 to 5 different preparations. Error bars indicate SEM. Data were fitted by the Hill equation with a coefficient of 3.

activity elicited in PN cell bodies. Cell bodies of PNs surround the antennal lobe in three discrete regions, the dorsal, ventral, or lateral cell clusters. The position of individual projection neurons within a cluster is not spatially stereotyped (Jefferis et al., 2001; Marin et al., 2002; Wong et al., 2002), and it is therefore difficult to identify the location of specific PNs innervating a given glomerulus. Figure 7 shows the imaging of PN cell bodies in the dorsal cluster in response to hexane and pyridine alone or to a mixture of the two odorants. Pyridine and hexane each activate 4–5 cell bodies in the dorsal cluster, which consists of 41 PNs (Wong et al., 2002). The response

to the mixture of the two odorants is additive: all PNs activated with a single odorant are also activated with the mixture and no novel PN cell bodies are observed. Thus, the response we observed in cell bodies, which is likely to result from spike propagation, reflects the pattern of glomerular activity.

### The Specificity of Glomerular Responses Reflects the Specificity of Odorant Receptor Sensitivity

Most sensory neurons in the fly antenna express *Or83b*, along with only one of the remaining odorant receptor genes. Neurons expressing a given odorant receptor gene project to one (or rarely two) discrete glomeruli within the antennal lobe. We have asked whether the odor-evoked activity profile for a given glomerulus directly reflects the responsivity of an individual odorant receptor.

The DA4 glomerulus receives input from sensory neurons expressing *Or43a*. Our imaging studies in which G-CaMP is expressed in either sensory axons or PN dendrites demonstrate that the DA4 glomerulus is activated by a characteristic panel of odors, including iso-amyl acetate, hexane, cineole, and several other odors (Figures 3 and 8). The VA1Im glomerulus is innervated by sensory neurons expressing *Or47b* (Vosshall et al., 2000) but this glomerulus does not respond to any of the odors tested in our series. We have misexpressed *Or43a* in neurons that express *Or47b* by generating transgenic flies bearing *Or47b-Gal4*, *UAS-Or43a*, and *UAS-GCaMP*. In these strains, *Or43a* is expressed in neurons that project to the native DA4 glomerulus and is ectopically expressed in *Or47b* neurons that innervate the VA1Im glomerulus. Imaging analysis of the VA1Im glomerulus in these strains reveals that the misexpression of *Or43a* confers upon the VA1Im glomerulus the odor response profile normally exhibited by the DA4 glomerulus (Figure 8C). Moreover, the kinetics of odor response in the VA1Im glomerulus in flies misexpressing *Or43a* closely resembles the kinetics of the native DA4 glomerulus (Figure 8B). Thus, the responsivity we observe upon imaging is a direct consequence of the nature of the odorant receptor expressed in a given sensory neuron such that the specificity of a glomerular response is determined by a single receptor.

## Discussion

### A Functional Map of Odor Activity

The organization of the peripheral olfactory system appears remarkably similar in fruit flies and mammals. The convergence of like axons into discrete glomerular structures provides an anatomic map in the antennal lobe (Gao et al., 2000; Vosshall et al., 2000; Scott et al., 2001). The quality of an odorant may therefore be reflected by defined spatial patterns of activity, first in the antennal lobe and ultimately in higher olfactory centers in the brain. Such a model postulates the convergence of information from deconstructed patterns in the antennal lobe to hierarchical cell assemblies in the protocerebrum and mushroom body. The identification of a spatially invariant sensory map in the fly protocerebrum that is divergent and no longer exhibits the insular segregation of like axons observed in the antennal lobe

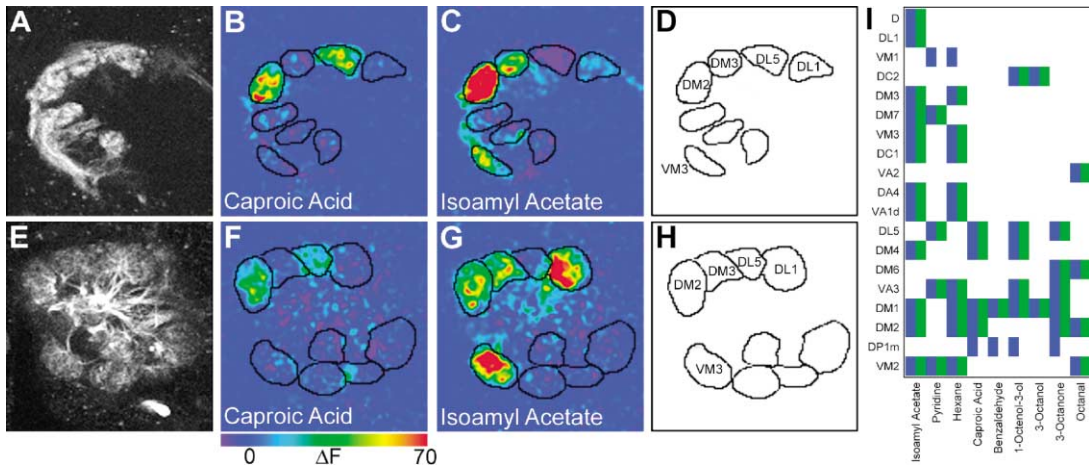


Figure 6. Similar Patterns of Glomerular Activation Are Observed upon Imaging Sensory Neuron Axons and Projection Neuron Dendrites (A–D) An optical plane revealing the DM2, DM3, DL5, DL1, and VM3 glomeruli of the antennal lobe is shown from a fly bearing the *Or83b-Gal4* and the *UAS-GCaMP* transgenes. These flies express G-CaMP in sensory neurons. (A) An image obtained prior to odor stimulation reveals the glomerular structure. The DL1 glomerulus is weakly labeled by *Or83b-Gal4*. Glomerular activity in response to caproic acid (B) and isoamyl acetate (C). Odor concentrations were 33% SV. (D) A schematic of identified glomeruli in this optical plane. (E–H) An optical plane revealing the DM2, DM3, DL5, DL1, and VM3 glomeruli of the antennal lobe is shown from a fly bearing the *GH146-Gal4* and the *UAS-GCaMP* transgenes. These flies express G-CaMP in projection neurons. (E) The glomerular structure shown in grayscale. Glomerular activity in response to caproic acid (F) and isoamyl acetate (G). Odor concentrations were 33% SV. (H) A schematic of identified glomeruli in this optical plane. (I) Concordance of glomerular responses in flies expressing G-CaMP in sensory neurons and projection neurons. Nine odorants at 36% SV were applied to preparations of flies bearing the *Or83b-Gal4* (green rectangles) and *UAS-GCaMP* transgenes. Each glomerulus that showed at least 20%  $\Delta F/F$  in G-CaMP labeled PNs (blue rectangles) in response to less than 20% SV for each odor was also activated in flies in which sensory neurons were labeled with G-CaMP. The VM1 and DP1m glomeruli are not labeled by *Or83b-Gal4*.

is consistent with these suggestions for it affords an opportunity for the integration of multiple glomerular inputs (Marin et al., 2002; Wong et al., 2002).

In this study, we have examined the relationship between the anatomic map and the functional representation of olfactory information in the brain. An understanding of the logic of odor perception requires functional analysis to identify odor-evoked patterns of activity in

neural assemblies and ultimately the relevance of these patterns to odor discrimination. We have developed an imaging system in *Drosophila* in which olfactory sensory neurons and projection neurons remain responsive to odors for up to five hours. We have coupled two-photon microscopy with the specific expression of calcium-sensitive fluorescent G-CaMP to obtain images of activity in both the glomeruli and cell bodies of the projection

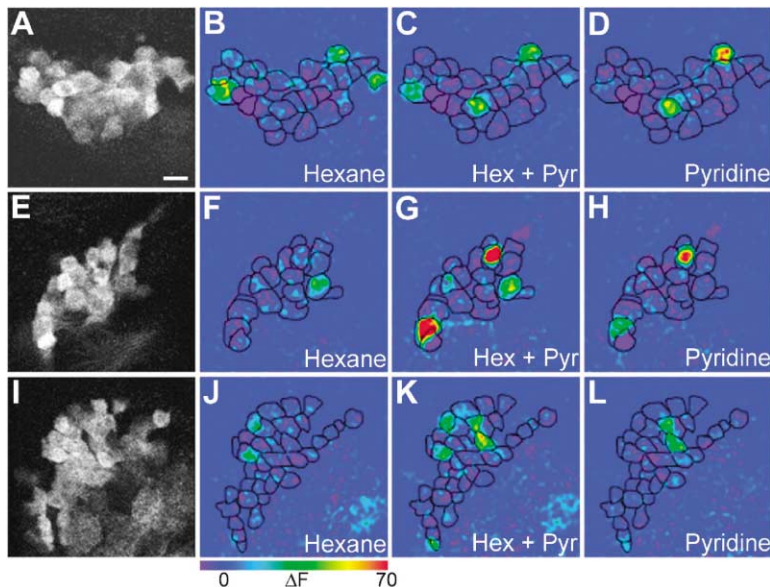


Figure 7. The Activity in PN Cell Bodies in Response to Odors

Cell bodies of *GH146-Gal4* positive PNs surround the antennal lobe in three discrete regions, the dorsal, ventral, and the lateral clusters. Pyridine and hexane at 20% SV each activate 4–5 cell bodies ( $n = 3$ ) in the dorsal cluster that contains 41 PN cell bodies. Images of the dorsal PN cell bodies from 3 different specimens are shown in different rows. (A, E, and I) Images of the dorsal cluster shown in grayscale prior to odor exposure. (B, F, and J) Peak response to hexane. (D, H, and L) Peak response to pyridine. (C, G, and K) Peak response to the mixture of hexane and pyridine. Scale bar = 10  $\mu\text{m}$ .

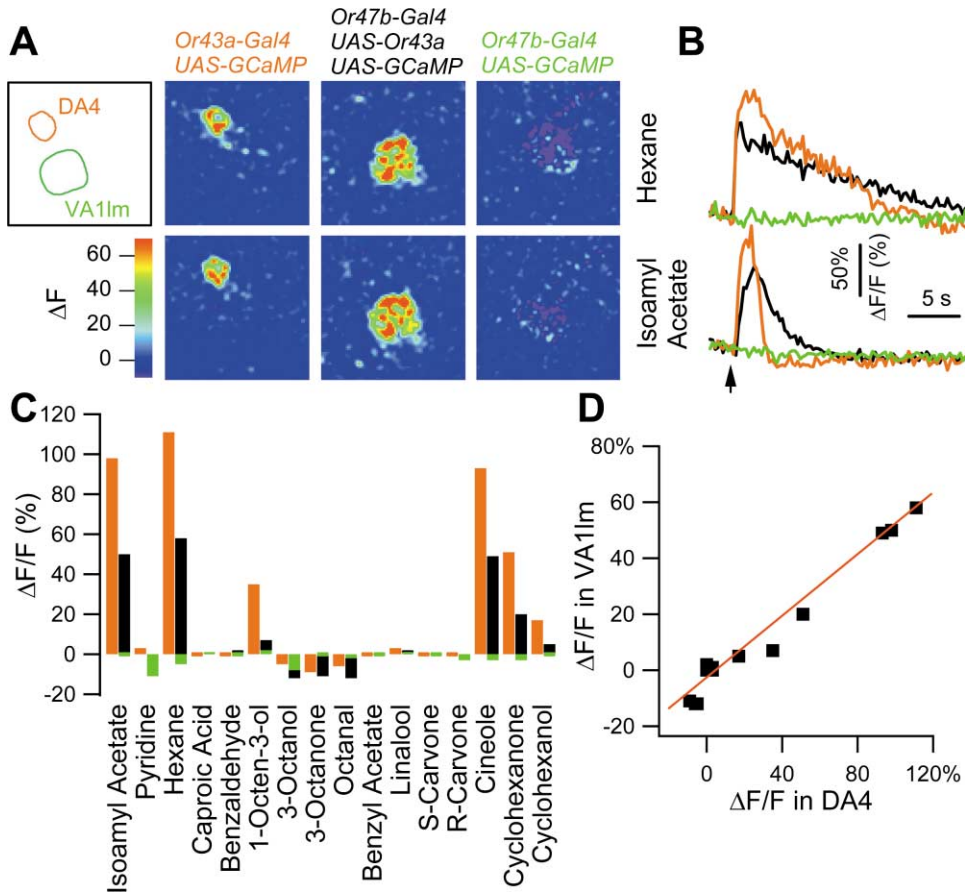


Figure 8. Glomerular Responsivity Is Determined by a Single Odorant Receptor

The DA4 glomerulus receives axons from sensory neurons expressing *Or43a*. The promoter of the *Or43a* gene was used to create an *Or43a-Gal4* transgene. In transgenic flies harboring the *Or43a-Gal4* transgene along with *UAS-GCaMP*, only the DA4 glomerulus is labeled with G-CaMP. The VA1Im glomerulus receives axons from sensory neurons expressing *Or47b*. Only the VA1Im glomerulus is labeled by G-CaMP in the fly bearing the *Or47b-Gal4* and *UAS-GCaMP* transgenes.  $\Delta F/F$  was measured at the DA4 glomerulus for the native *Or43a*, and at the VA1Im glomerulus for the native *Or47b* and the misexpressed *Or43a*.

(A) Misexpression of *Or43a* in the sensory neurons normally expressing the *Or47b* gene confers upon the VA1Im glomerulus the same characteristic odor response profile as the DA4 glomerulus. Images of peak  $\Delta F$  response to hexane and isoamyl acetate at 40% SV are shown. (B) Time course of  $\Delta F/F$  in response to hexane and isoamyl acetate for the misexpressed *Or43a* (black traces), the native *Or43a* (red traces), and the native *Or47b* (green traces).

(C) Peak  $\Delta F/F$  in response to 16 different odors at 40% SV for the native *Or43a* (red bars), the misexpressed *Or43a* (black bars), and native *Or47b* (green bars). Each  $\Delta F/F$  value represents the averaged response from three different animals.

(D) Peak  $\Delta F/F$  values for the misexpressed *Or43a* are plotted against those for the native *Or43a* in response to the same odor. The linear regression line reveals that odor response profile of the misexpressed receptor is similar to that of the native receptor.

neurons in the antennal lobe. We observe fluorescence intensity changes as large as 120% in specific glomeruli when odor is applied at high concentration to the antennae. Moreover, the high signal-to-noise ratio permits analysis over a broad range of odor concentrations that are likely to approximate those encountered in nature. Experiments to correlate fluorescence changes with electrical activity suggest that our imaging technique readily detects a glomerular signal from a single action potential in as few as 20 incoming sensory axons.

This imaging technique has allowed us to measure the responsiveness of 23 glomeruli to 16 different odors with a sensitivity and spatiotemporal resolution not previously possible. We observe that all odors tested (with the exception of S- and R-carvone) elicit different patterns of glomerular activity that are conserved in multiple

flies. Moreover, identical patterns are observed whether we image activity in sensory axons or the dendrites of projection neurons. At physiological concentrations of odors, the map is sparse with most glomeruli responsive to a small subset of odors. Higher odor concentrations, necessarily employed in less sensitive imaging approaches, recruit larger numbers of glomeruli. Finally, the specific responsiveness of a given glomerulus is a consequence of the specificity of a single odorant receptor expressed by the incoming sensory neurons. The ability to completely and faithfully transfer responsiveness by the misexpression of a single receptor provides significant support for the “one neuron-one receptor” observation in which individual olfactory neurons in both vertebrates and insects express only a single receptor gene.

Several conclusions emerge from the analysis of odor

responses in genetically defined subpopulations of neurons. First, each odor elicits a distinct and sparse pattern of activity that is stereotyped in different flies. The pattern at physiological odor concentrations is characteristic and allows our brains to distinguish among odors without further mathematical analysis. The ability to identify distinct patterns of activity at natural odor concentrations suggests that the patterns we observe will reflect information recognized and used by the fly brain to discriminate odors. Second, the observation that the patterns of glomerular activity are similar upon imaging of sensory and projection neurons suggests the faithful transmission of sensory input to higher brain centers. These conclusions are supported by the summation of glomerular responses in PN cell bodies. We do not observe evidence for excitatory or inhibitory integration events that significantly alter the spatial character of the map (see below). Third, the response patterns of given glomerulus is solely a function of the specificity of a single odorant receptor, a finding consistent with prior molecular and anatomic studies that reveal that neurons express only a single receptor and like axons converge on a single glomerulus.

The character of the functional map in the fly is consistent with previous studies that have monitored odor-evoked patterns of neural activity by electrical recording and other imaging techniques. Electrical recordings of odor-evoked responses combine high sensitivity with temporal resolution in the submillisecond range to define the response of projection neurons to different odors (Imamura et al., 1992; Laurent and Naraghi, 1994; Yokoi et al., 1995). This approach is limited by the inability to sample more than a few cells at different locations in different organisms. Neural imaging techniques are capable of analyzing odor-evoked neural activity in large populations of neurons. Changes in 2-deoxyglucose uptake (Stewart et al., 1979; Jourdan et al., 1980; Rodrigues, 1988; Johnson and Leon, 2000) and c-Fos expression (for review see Guthrie and Gall, 1995) correlate with odor stimulation and reveal the activation of specific glomeruli by specific odors. However, it is difficult to determine the sensitivity of these techniques, temporal resolution is poor and only a single odor can be sampled in a given organism. Intrinsic optical imaging in the mammalian olfactory bulb reveals correlation between electrical activity and the intrinsic optical signal (Luo and Katz, 2001) and identifies activity in specific glomeruli in response to different odors (Rubin and Katz, 1999; Uchida et al., 2000; Meister and Bonhoeffer, 2001; Beluscio et al., 2002). However, low spatial resolution and the inability to perform optical sectioning restrict image resolution to small exposed surfaces of the bulb.

Microscopic imaging of fluorescent changes in  $\text{Ca}^{2+}$ -sensitive dyes (Grynkiewicz et al., 1985) provides far greater signal-to-noise ratio and greater sensitivity. Fluorescent microscopy can detect changes in fluorescent intensity with excellent spatial and temporal resolution and has permitted the demonstration of odor-evoked patterns in the olfactory bulb of vertebrates and the antennal lobe of insects (Friedrich and Korsching, 1997; Joerges et al., 1997; Galizia et al., 1999; Wachowiak and Cohen, 2001).  $\text{Ca}^{2+}$ -sensitive dyes however require the ability to uniformly load cells, a procedure that may be difficult in many brain regions and most often does not

permit sampling of specific neuronal populations. Recently, imaging studies with synapto-pHluorin, a fluorescent indicator of pH change, have revealed dense patterns of glomerular activity in the fly antennal lobe (Ng et al., 2002). This fluorescent indicator has been expressed in defined neurons and affords spatial resolution but has limited sensitivity due to low signal-to-noise ratio. As a consequence, analysis requires non-physiological concentrations that may result in spatial representations not naturally encountered by the fly brain. The imaging system we have developed couples the high sensitivity of G-CaMP (Nakai et al., 2001) with two-photon microscopy (Denk et al., 1990) to allow the detection of odor response at physiological concentrations. The use of G-CaMP allows sampling of genetically defined subpopulations of neurons, thereby permitting the delineation of the locus and source of neural activity with greater sensitivity and excellent spatial resolution.

### The Nature of the Functional Map

Despite the limitations inherent in all imaging approaches, a consistent picture has emerged which reveals that different odors activate spatially distinct glomeruli and their associated projection neurons. One interesting feature of the map in *Drosophila* is that it is sparse and only becomes dense at high odor concentrations. At concentrations of odor below 5%–10% saturated vapor, glomeruli are narrowly tuned and respond to a restricted range of molecular structures. At higher odor concentrations that are likely to exceed those encountered in natural environment, several glomeruli appear “promiscuous” and respond to multiple odors of widely different molecular structures. This dense map is unlikely to be generated in nature and these patterns will unlikely to be encountered by the fly brain outside of the laboratory. The differential sensitivity of different glomeruli to a given odor results in an increase in the number of active glomeruli with increasing odor concentration. This poses an interesting problem in perception for all sensory systems: how does the brain respond to different intensities of sensory input? In olfaction, the dynamic range of responsiveness to a given odor often is quite large and for many odors we expect that despite large concentration differences the quality of the odor percept and the behavioral response is likely to remain the same. If the quality of an odor is reflected in glomerular pattern, then this poses the problem of constancy of odor quality.

The sparseness of the response observed in fly contrasts with the redundant or promiscuous response observed in the mitral cells of zebrafish (Friedrich and Laurent, 2001) and PNs of locust (Perez-Orive et al., 2002). In locust, for example, extracellular recordings reveal that most PNs respond to most odors. This is in sharp contrast to PN responses we observe upon  $\text{Ca}^{2+}$  imaging in both PN dendrites and cell bodies. These differences may reflect the fact that in locust and zebrafish individual PNs innervate multiple glomeruli (Laurent and Naraghi, 1994; Friedrich and Laurent, 2001) whereas in the fly and in most vertebrates analyzed PNs innervate a single glomerulus (Stocker et al., 1990; Jefferis et al., 2001). These anatomic and functional differences might underlie a different logic of olfactory discrimination in

the two sets of organisms or technical distinctions in the measurements of activity that will ultimately resolve into a more unified mechanism.

One feature of the map in the vertebrate olfactory bulb is the juxtaposition of glomeruli responsive to structurally similar odorant molecules (Johnson and Leon, 2000; Uchida et al., 2000; Belluscio and Katz, 2001; Meister and Bonhoeffer, 2001). In the rabbit main olfactory bulb, aliphatic aldehydes for example activate a collection of neighboring glomeruli in the dorsal bulb (Yokoi et al., 1995; Mori et al., 1999). This close apposition of glomeruli with similar responsivity affords the opportunity for lateral inhibition (Mori et al., 1999; Sachse and Galizia, 2002), an olfactory version of “center-surround” in the visual system that may serve to sharpen the response and enhance discriminatory power. The clustering of glomeruli with similar odorant specificities is not observed in our imaging studies. If this mechanism of “lateral inhibition” is operating in *Drosophila*, it may exploit the specific connectivity of inhibitory interneurons that operate across longer relative distances rather than only on local interneuron circuits.

Our studies do not reveal modulation at glomerular synapses since the map we observe is qualitatively identical whether we image activity in the sensory axon termini or the dendrites at the projection neurons. Similar but more preliminary conclusions emerge from imaging analysis of the PN cell bodies in which responsivity to two odorants sums the individual responses to single odors. Thus, within the quantitative limitations of this sort of analysis, we argue that higher olfactory centers in the protocerebrum and mushroom body faithfully receive input imparted by excitation of the sensory neurons.

Finally, it is important to question whether the responses observed in our imaging analysis of the antennal lobe are physiologically relevant for odor discrimination by the organism. Our imaging approach, as in all other electrophysiological and imaging analyses, is limited by the sensitivity and breadth of the population of neurons that can be analyzed. Whereas the glomerular responses we observe clearly reflect specific responses to defined odors, we cannot with certainty determine whether the patterns of spatial activity we observe are salient and reflect the parameters employed by the protocerebrum to discriminate and respond to odors. The mere existence of a map, whether anatomic or functional, does not prove that spatial information is the underlying parameter of a code defining odor quality. It has been suggested that the quality of an odor is encoded not in topography, but by temporal dynamics, that different odors elicit different temporal patterns of activity and that this is a more relevant attribute of odor quality (Laurent, 1999). The development of a high-resolution imaging system that identifies a functional map of odor activity, coupled with genetic approaches to perturb the map, should permit an assessment of the significance of spatial coding for olfactory discrimination.

## Experimental Procedures

### Experimental Animals and Preparation

Flies were raised on standard medium at 25°C. To minimize background fluorescent intensity, adult flies were used for experiments

within 48 hr after eclosion. G-CaMP 1.3 (Nakai et al., 2001), kindly provided by Junichi Nakai, was inserted into the pUAST vector (Brand and Perrimon, 1993) via the BglII and NotI restriction sites. Two independent insertions at 7B7 and 18F1 on the X chromosome were recombined. Female flies carrying four copies of the G-CaMP transgenes were used for all imaging experiments to enhance fluorescent intensity. *UAS-Or43a* was constructed by inserting the 1.556 kb full-length *Or43a* cDNA (Vosshall et al., 1999) into the pUAST vector as an EcoRI/Asp718I fragment. *Or43a-Gal4* was constructed by first generating a 3.424 kb PCR product, corresponding to sequences immediately upstream of the ATG start codon of *Or43a*, from *Drosophila* genomic DNA. This putative *Or43a* promoter fragment was cloned into the NotI site of the pCasperAUG-Gal4-X vector (Vosshall et al., 2000). *Or83b-Gal4* was constructed by first generating a 2.642 kb PCR product, corresponding to sequences immediately upstream of the ATG start codon of *Or83b*, from *Drosophila* genomic DNA. This putative *Or83b* promoter fragment was cloned into the Asp718I site of the pCasperAUG-VP22-Gal4 vector, which carries a fusion of VP22 to Gal4, a modification that does not affect the activity of Gal4 (Vosshall et al., 2000). Antennal expression patterns of both *Or43a-Gal4* and *Or83b-Gal4* were confirmed with in situ hybridization. *Or47b-Gal4* (Vosshall et al., 2000), *Or43a-Gal4*, *Or83b-Gal4*, and *GH146-Gal4* (Stocker et al., 1997) were used to drive the expression of *UAS-GCaMP* or *UAS-Or43a*.

The osmolarity of adult *Drosophila* hemolymph is 250 mOsm (Singleton and Woodruff, 1994). An adult hemolymph like (abbreviated as AHL) saline containing 108 mM NaCl, 5 mM KCl, 2 mM CaCl<sub>2</sub>, 8.2 mM MgCl<sub>2</sub>, 4 mM NaHCO<sub>3</sub>, 1 mM NaH<sub>2</sub>PO<sub>4</sub>, 5 mM trehalose, 10 mM sucrose, 5 mM HEPES [pH 7.5, 265 mOsm] was used for all imaging experiments. Neuronal morphology was normal and good intracellular recording was obtained from projection neurons with the AHL saline (data not shown).

An antennae-brain preparation was obtained by microdissection of decapitated flies to remove head cuticle and connective tissues. Neural activity of the fly brain was reduced by dissecting in Ca<sup>2+</sup>-free AHL saline. The preparation was pinned down on a thin Sylgard slab with fine tungsten wires, rinsed in AHL saline, and embedded with 2% agarose gel (Sigma type VII-A) in AHL saline warmed to 37°C. Prior to imaging, the agarose covering the antennae was removed to allow exposure to odor and a glass cover slip was used to cover the brain region. Maxillary palps and all other sensory structures were removed, leaving the third antennal segment as the only organ providing sensory input to the antennal lobe. This preparation could respond to odor stimulation for up to five hours.

### Odor Stimulation

The olfactometer employed was a modification of the design described in Dethier and Yost (1952). It permitted quantitative control of odor stimulation by diluting saturated vapor concentration up to a 1:300 ratio. Two digital peristaltic pumps (Ismatec SA, Glattbrugg-Zurich, Switzerland), a four-channel solenoid valve controller system (Series 18, Parker Hannifin Corporation, Fairfield, NJ), disposable 15 ml serum vials and luer tubings (21G Vacutainer, Becton Dickinson, Franklin Lakes, NJ) were used to construct the olfactometer. Two independent humidified air streams were generated from the two peristaltic pumps. One air stream went into the solenoid valve system, which could be switched from an empty vial (air) to one of the three vials that each contained 300 μl odorant and then back to the empty vial on cessation of the stimulation. The constant airflow before, during, and after the 2 s odor stimulation ensured minimum mechanical change for odor stimulation. The other air stream was used to dilute the saturated vapor and the sum of flow rates for the two airstreams was kept constant at 90 ml/min. When a new odor was used in the system all tubings and vials downstream of the solenoid valves were replaced to eliminate any potential contamination from previously used odors. All odors were obtained from Sigma-Aldrich/Fluka of the highest purity available.

The tip of the olfactometer was positioned about 10 mm away from the antennae of the brain preparation in imaging experiments, which should inevitably result in a further dilution of the odor concentration at the tip due to diffusion. Oxygen, instead of an odorant, was taken into the olfactometer to estimate the odor concentration arriving at the antennae and an oxygen meter (ISO2, World Precision

Instruments, Sarasota, FL) was used for this measurement. The oxygen concentration at the position of the antennae was only 40% of the value calculated from the dilution ratio of the olfactometer. The factor of 40% was therefore applied to all odor concentration calculations.

#### Two-Photon Microscopy and Data Analysis

Calcium imaging was performed with a two-photon microscope (Denk et al., 1990), which was custom built from off the shelf components similar to that described in Denk et al. (1994). The upright fixed stage microscope was assembled onto an optical rail, which sits on a X-Y motorized stage (Kollmorgen, Lawrence, MA) controlled by a modified MP285 driver (Sutter Instrument, Novato, CA). A stepping motor (PK245-01AA, Oriental Motor, Clifton, NJ), also controlled by the modified MP285 driver, was used to move the objective lens (Achromplan IR 40 $\times$ /0.80NA, Carl Zeiss, Thornwood, NY) in the vertical direction.

The light source was a Mira 900 titanium:sapphire laser, pumped by a Verdi 10-W solid-state laser (Coherent, Santa Clara, CA). Mode-locked laser output had an ultra-short pulse width of <200 fs at a repetition rate of  $\sim$ 76 MHz. The laser power for sample excitation was attenuated by the rotation of a Z-cut quartz plate (CVI Laser Corporation, Albuquerque, NM), which rotated the polarization direction of the laser beam that passes through a polarizing beamsplitter cube (New Focus, San Jose, CA). Excitation laser light of  $\sim$ 930 nm wavelength produced less background fluorescence than other shorter wavelengths. Laser beam scanning was controlled by a pair of galvanometer 3 mm mirrors (Model 6210, Cambridge Technology, Cambridge, MA) driven by custom software CfNT (version 1.528), kindly provided by Winfried Denk. The scan mirrors were  $\sim$ 3 mm away from the exit window of the laser and were the limiting aperture of the expanded laser beam. This is the largest mirror that affords a scan rate better than 500 Hz. A dichroic mirror (595DCXR), allowing infrared laser beam to pass and reflect visible photons, was placed on top of a binocular phototube (Carl Zeiss, Thornwood, NY) between the scan lens and the tube lens. This configuration of whole area detection permits more photon collection than the scheme of descanned detection (Denk et al., 1994). A blocking filter (E700SP-special) and a band-pass filter (HQ525/50 m, for two-photon application) were inserted between the focusing lens and the PMT light detector (R3896 in conjunction with a C6270 socket, Hamamatsu Photonics, Bridgewater, NJ) to select for the emission spectrum of G-CaMP (peak at 509 nm, Nakai et al., 2001). All optical filters were from Chroma Technology Corporation (Brattleboro, VT). Protected silver-coated mirrors (New Focus, San Jose, CA) were used for beam reflection.

Data acquisition was performed with CfNT software (version 1.528) on a 500 MHz Pentium II computer equipped with an imaging board (XPG-1000, Coreco, Ottawa, Canada) and a Fulcrum data acquisition board (DT3809, Marlboro, MA) to interface with external devices including shutter, scanning mirrors, XYZ stepping motors, and light detectors.

Images were acquired at  $\sim$ 4 frames per second (256 ms per frame) with a resolution of 128  $\times$  128 pixels (0.75  $\times$  0.75  $\mu$ m for each pixel). For each odor stimulation, 100 frames were acquired. After all odor stimulations were finished, a high-resolution image stack of the antennal lobe at 512  $\times$  512 pixels (1  $\mu$ m step) was acquired for glomerular identification. ImageJ (version 1.26t, available from NIH) and a custom plug-in were used to compute  $\Delta F/F$  and to identify glomeruli. A Gaussian convolution filter with radius of 2 was applied to all  $\Delta F$  images presented. Igor Pro (version 4.0, Wavemetrics, Lake Oswego, OR) and a custom procedure were used for quantitative analysis of odor response. Glomeruli were identified anatomically according to the previous established antennal lobe map (Laissue et al., 1999). DM7, the dorsal lateral neighbor of the DM6 glomerulus, was identified in this study.

#### Acknowledgments

We thank Junichi Nakai and Keiji Imoto for providing the G-CaMP construct and Reinhard Stocker for providing the *GH146-Gal4* fly line. We also thank Winfried Denk for continual advice on two-photon imaging; Fritjof Helmchen, Michael Müller, Ray Stepnoski,

Jürgen Tritthardt, and Chris Xu for technical assistance with setting up the two-photon microscope; Phyllis Kisloff for assistance in preparing the manuscript; and Atsuko Adachi for fly injection. We thank Yi Zhong and Yalin Wang for open communication of data during the course of these studies. We thank Tom Jessell, Larry Katz, Sam Wang, Rafa Yuste, and members of the Axel Lab for critical comments on the manuscript. This research was supported by the Howard Hughes Medical Institute (R.A.) and by grants from the National Institutes of Health (NIMH) MH50733 (R.A., J.W.W., and A.M.W.), the National Science Foundation IBN-0092693 (L.B.V.), and the Mathers Foundation (R.A.).

Received: October 30, 2002

Revised: December 18, 2002

#### References

- Belluscio, L., and Katz, L.C. (2001). Symmetry, stereotypy, and topography of odorant representations in mouse olfactory bulbs. *J. Neurosci.* 21, 2113–2122.
- Belluscio, L., Lodovichi, C., Feinstein, P., Mombaerts, P., and Katz, L.C. (2002). Odorant receptors instruct functional circuitry in the mouse olfactory bulb. *Nature* 419, 296–300.
- Brand, A.H., and Perrimon, N. (1993). Targeted gene expression as a means of altering cell fates and generating dominant phenotypes. *Development* 118, 401–415.
- Clyne, P.J., Warr, C.G., Freeman, M.R., Lessing, D., Kim, J., and Carlson, J.R. (1999). A novel family of divergent seven-transmembrane proteins: candidate odorant receptors in *Drosophila*. *Neuron* 22, 327–338.
- de Bruyne, M., Foster, K., and Carlson, J.R. (2001). Odor coding in the *Drosophila* antenna. *Neuron* 30, 537–552.
- Delaney, K., Davison, I., and Denk, W. (2001). Odour-evoked [Ca<sup>2+</sup>] transients in mitral cell dendrites of frog olfactory glomeruli. *Eur. J. Neurosci.* 13, 1658–1672.
- Denk, W., Strickler, J.H., and Webb, W.W. (1990). Two-photon laser scanning fluorescence microscopy. *Science* 248, 73–76.
- Denk, W., Delaney, K.R., Gelperin, A., Kleinfeld, D., Strowbridge, B.W., Tank, D.W., and Yuste, R. (1994). Anatomical and functional imaging of neurons using 2-photon laser scanning microscopy. *J. Neurosci. Methods* 54, 151–162.
- Dethier, V.G., and Yost, M.T. (1952). Olfactory stimulation of blowflies by homologous alcohols. *J. Gen. Physiol.* 35, 823–839.
- Dunipace, L., Meister, S., McNealy, C., and Amrein, H. (2001). Spatially restricted expression of candidate taste receptors in the *Drosophila* gustatory system. *Curr. Biol.* 11, 822–835.
- Friedrich, R.W., and Korsching, S.I. (1997). Combinatorial and chemotopic odorant coding in the zebrafish olfactory bulb visualized by optical imaging. *Neuron* 18, 737–752.
- Friedrich, R.W., and Laurent, G. (2001). Dynamic optimization of odor representations by slow temporal patterning of mitral cell activity. *Science* 291, 889–894.
- Galizia, C.G., Sachse, S., Rappert, A., and Menzel, R. (1999). The glomerular code for odor representation is species specific in the honeybee *Apis mellifera*. *Nat. Neurosci.* 2, 473–478.
- Gao, Q., and Chess, A. (1999). Identification of candidate *Drosophila* olfactory receptors from genomic DNA sequence. *Genomics* 60, 31–39.
- Gao, Q., Yuan, B., and Chess, A. (2000). Convergent projections of *Drosophila* olfactory neurons to specific glomeruli in the antennal lobe. *Nat. Neurosci.* 3, 780–785.
- Grynkiewicz, G., Poenie, M., and Tsien, R.Y. (1985). A new generation of Ca<sup>2+</sup> indicators with greatly improved fluorescence properties. *J. Biol. Chem.* 260, 3440–3450.
- Guthrie, K.M., and Gall, C.M. (1995). Functional mapping of odor-activated neurons in the olfactory bulb. *Chem. Senses* 20, 271–282.
- Helmchen, F., Svoboda, K., Denk, W., and Tank, D.W. (1999). In vivo dendritic calcium dynamics in deep-layer cortical pyramidal neurons. *Nat. Neurosci.* 2, 989–996.

- Imamura, K., Mataga, N., and Mori, K. (1992). Coding of odor molecules by mitral/tufted cells in rabbit olfactory bulb. I. aliphatic compounds. *J. Neurophysiol.* *68*, 1986–2002.
- Jefferis, G.S., Marin, E.C., Stocker, R.F., and Luo, L. (2001). Target neuron prespecification in the olfactory map of *Drosophila*. *Nature* *414*, 204–208.
- Joerges, J., Kuttner, A., Galizia, C.G., and Menzel, R. (1997). Representations of odours and odour mixtures visualized in the honeybee brain. *Nature* *387*, 285–287.
- Johnson, B.A., and Leon, M. (2000). Modular representations of odorants in the glomerular layer of the rat olfactory bulb and the effects of stimulus concentration. *J. Comp. Neurol.* *422*, 496–509.
- Jourdan, F., Duveau, A., Astic, L., and Holley, A. (1980). Spatial distribution of [<sup>14</sup>C]2-deoxyglucose uptake in the olfactory bulbs of rats stimulated with two different odours. *Brain Res.* *188*, 139–154.
- Kauer, J.S., Senseman, D.M., and Cohen, L.B. (1987). Odor-elicited activity monitored simultaneously from 124 regions of the salamander olfactory bulb using a voltage-sensitive dye. *Brain Res.* *418*, 255–261.
- Laisue, P.P., Reiter, C., Hiesinger, P.R., Halter, S., Fischbach, K.F., and Stocker, R.F. (1999). Three-dimensional reconstruction of the antennal lobe in *Drosophila melanogaster*. *J. Comp. Neurol.* *405*, 543–552.
- Laurent, G. (1999). A systems perspective on early olfactory coding. *Science* *286*, 723–728.
- Laurent, G., and Naraghi, M. (1994). Odorant-induced oscillations in the mushroom bodies of the locust. *J. Neurosci.* *14*, 2993–3004.
- Luo, M., and Katz, L.C. (2001). Response correlation maps of neurons in the mammalian olfactory bulb. *Neuron* *32*, 1165–1179.
- Malnic, B., Hirono, J., Sato, T., and Buck, L.B. (1999). Combinatorial receptor codes for odors. *Cell* *96*, 713–723.
- Marin, E.C., Jefferis, G.S., Komiyama, T., Zhu, H., and Luo, L. (2002). Representation of the glomerular olfactory map in the *Drosophila* brain. *Cell* *109*, 243–255.
- Meister, M., and Bonhoeffer, T. (2001). Tuning and topography in an odor map on the rat olfactory bulb. *J. Neurosci.* *21*, 1351–1360.
- Miyawaki, A., Llopis, J., Heim, R., McCaffery, J.M., Adams, J.A., Ikura, M., and Tsien, R.Y. (1997). Fluorescent indicators for Ca<sup>2+</sup> based on green fluorescent proteins and calmodulin. *Nature* *388*, 882–887.
- Mombaerts, P. (1999). Molecular biology of odorant receptors in vertebrates. *Annu. Rev. Neurosci.* *22*, 487–509.
- Mori, K., Nagao, H., and Yoshihara, Y. (1999). The olfactory bulb: coding and processing of odor molecule information. *Science* *286*, 711–715.
- Nakai, J., Ohkura, M., and Imoto, K. (2001). A high signal-to-noise Ca<sup>2+</sup> probe composed of a single green fluorescent protein. *Nat. Biotechnol.* *19*, 137–141.
- Ng, M., Roorda, R.D., Lima, S.Q., Zemelman, B.V., Morcillo, P., and Miesenböck, G. (2002). Transmission of olfactory information between three populations of neurons in the antennal lobe of the fly. *Neuron* *36*, 463–474.
- Perez-Orive, J., Mazor, O., Turner, G.C., Cassenaer, S., Wilson, R.I., and Laurent, G. (2002). Oscillations and sparsening of odor representations in the mushroom body. *Science* *297*, 359–365.
- Rodrigues, V. (1988). Spatial coding of olfactory information in the antennal lobe of *Drosophila melanogaster*. *Brain Res.* *453*, 299–307.
- Rubin, B.D., and Katz, L.C. (1999). Optical imaging of odorant representations in the mammalian olfactory bulb. *Neuron* *23*, 499–511.
- Sachse, S., and Galizia, C.G. (2002). Role of inhibition for temporal and spatial odor representation in olfactory output neurons: a calcium imaging study. *J. Neurophysiol.* *87*, 1106–1117.
- Scott, K., Brady, R., Jr., Cravchik, A., Morozov, P., Rzhetsky, A., Zuker, C., and Axel, R. (2001). A chemosensory gene family encoding candidate gustatory and olfactory receptors in *Drosophila*. *Cell* *104*, 661–673.
- Singleton, K., and Woodruff, R.I. (1994). The osmolarity of adult *Drosophila* hemolymph and its effect on oocyte-nurse cell electrical polarity. *Dev. Biol.* *161*, 154–167.
- Spors, H., and Grinvald, A. (2002). Spatio-temporal dynamics of odor representations in the mammalian olfactory bulb. *Neuron* *34*, 301–315.
- Stewart, W.B., Kauer, J.S., and Shepherd, G.M. (1979). Functional organization of rat olfactory bulb analysed by the 2-deoxyglucose method. *J. Comp. Neurol.* *185*, 715–734.
- Stocker, R.F. (1994). The organization of the chemosensory system in *Drosophila melanogaster*: a review. *Cell Tissue Res.* *275*, 3–26.
- Stocker, R.F., Lienhard, M.C., Borst, A., and Fischbach, K.F. (1990). Neuronal architecture of the antennal lobe in *Drosophila melanogaster*. *Cell Tissue Res.* *262*, 9–34.
- Stocker, R.F., Heimbeck, G., Gendre, N., and de Belle, J.S. (1997). Neuroblast ablation in *Drosophila* P[GAL4] lines reveals origins of olfactory interneurons. *J. Neurobiol.* *32*, 443–456.
- Svoboda, K., Denk, W., Kleinfeld, D., and Tank, D.W. (1997). In vivo dendritic calcium dynamics in neocortical pyramidal neurons. *Nature* *385*, 161–165.
- Uchida, N., Takahashi, Y.K., Tanifuji, M., and Mori, K. (2000). Odor maps in the mammalian olfactory bulb: domain organization and odorant structural features. *Nat. Neurosci.* *3*, 1035–1043.
- Vosshall, L.B. (2000). Olfaction in *Drosophila*. *Curr. Opin. Neurobiol.* *10*, 498–503.
- Vosshall, L.B., Amrein, H., Morozov, P.S., Rzhetsky, A., and Axel, R. (1999). A spatial map of olfactory receptor expression in the *Drosophila* antenna. *Cell* *96*, 725–736.
- Vosshall, L.B., Wong, A.M., and Axel, R. (2000). An olfactory sensory map in the fly brain. *Cell* *102*, 147–159.
- Wachowiak, M., and Cohen, L.B. (2001). Representation of odorants by receptor neuron input to the mouse olfactory bulb. *Neuron* *32*, 723–735.
- Wang, S.S.-H., Denk, W., and Hausser, M. (2000). Coincidence detection in single dendritic spines mediated by calcium release. *Nat. Neurosci.* *3*, 1266–1273.
- Wang, J.W., Denk, W., Flores, J., and Gelperin, A. (2001). Initiation and propagation of calcium-dependent action potentials in a coupled network of olfactory interneurons. *J. Neurophysiol.* *85*, 977–985.
- Wong, A.M., Wang, J.W., and Axel, R. (2002). Spatial representation of the glomerular map in the *Drosophila* protocerebrum. *Cell* *109*, 229–241.
- Yokoi, M., Mori, K., and Nakanishi, S. (1995). Refinement of odor molecule tuning by dendrodendritic synaptic inhibition in the olfactory bulb. *Proc. Natl. Acad. Sci. USA* *92*, 3371–3375.
- Yuste, R., and Denk, W. (1995). Dendritic spines as basic functional units of neuronal integration. *Nature* *375*, 682–684.